

Relative importance of electrostatic and van der Waals forces in particle adhesion to rough conducting surfaces

Siddharth Rajupet ¹, Adriaan A. Riet ¹, Qizan Chen,¹ Mamadou Sow,² and Daniel J. Lacks ^{1,*}

¹*Department of Chemical and Biomolecular Engineering, Case Western Reserve University, Cleveland, Ohio 44106, USA*

²*Institut de Radioprotection et de Sûreté Nucléaire (IRSN), PSN-RES/SCA, Gif-sur-Yvette, 91192, France*



(Received 4 February 2021; revised 3 April 2021; accepted 6 April 2021; published 30 April 2021)

It is commonly assumed that van der Waals forces dominate adhesion in dry systems and electrostatic forces are of second order importance and can be safely neglected. This is unambiguously the case for particles interacting with flat surfaces. However, all surfaces have some degree of roughness. Here we calculate the electrostatic and van der Waals contributions to adhesion for a polarizable particle contacting a rough conducting surface. For van der Waals forces, surface roughness can diminish the force by several orders of magnitude. In contrast, for electrostatic forces, surface roughness affects the force only slightly, and in some regimes it actually increases the force. Since van der Waals forces decrease far more strongly with surface roughness than electrostatic forces, surface roughness acts to increase the relative importance of electrostatic forces to adhesion. We find that for a particle contacting a rough conducting surface, electrostatic forces can be dominant for particle sizes as small as $\sim 1\text{--}10\ \mu\text{m}$.

DOI: [10.1103/PhysRevE.103.042906](https://doi.org/10.1103/PhysRevE.103.042906)

I. INTRODUCTION

Particle adhesion to conducting surfaces is of broad concern in industrial systems where particles can stick to the metal walls of reactors [1–3], pipes [4,5], etc. [6,7]. We are particularly interested in dust adhesion in Tokamak fusion reactors, where the adhesion of oxide coated particles to reactor walls prevents dissemination of radiologically and chemically hazardous dust into the environment during loss of vacuum scenarios [8–10]. Adhesion in dry systems is governed by two force contributions: van der Waals (vdW) forces and electrostatic forces. It is generally taken that vdW forces dominate particle adhesion, and that electrostatic forces are insignificant and can be neglected even when the particle is highly charged [11–14].

As the simplest example, consider the adhesion forces between two flat infinite surfaces with equal and opposite charge. The van der Waals force per area, a , is given by $F_V^S/a = H/6\pi d^3$ [15], and the electrostatic force per area is given by $F_E^S/a = \sigma^2/2\epsilon_0$ [16], where H is the Hamaker constant, σ is the surface charge density, ϵ_0 is the permittivity of vacuum, and d is the separation between the surfaces. The value of H is typically $H \sim 10^{-19}\ \text{J}$, and the value of σ for a highly charged surface is $\sigma \sim 10^{-5}\ \text{C/m}^2$. Using these values, the vdW force between these surfaces at contact ($d \approx 0.5\ \text{nm}$) is more than a million times larger than the electrostatic force—clearly the electrostatic force is in fact negligible here.

For the more relevant case of a particle interacting with a surface, a similar conclusion holds. Consider the forces acting on a nondeforming particle in contact with a flat conducting surface (the interaction of a nondeforming particle is the Derjaguin, Muller, Toporov (DMT) limit in particle adhesion).

The vdW force on a spherical particle with radius R separated from a flat surface by distance d is given by [15],

$$F_V^S = \frac{HR}{6d^2}. \quad (1)$$

The electrostatic attractive force for a nonpolarizable sphere with radius R and uniform surface charge density σ interacting with a smooth conducting surface is equivalent to the Coulombic force between two spheres of equal and opposite charge separated by distance $2d$ [16],

$$F_E^S = \frac{\pi\sigma^2 R^4}{\epsilon_0(d+R)^2}. \quad (2)$$

Using the same H and σ from above, the vdW force on a $1\text{-}\mu\text{m}$ radius particle in contact with a flat conducting surface (such that $d \approx 0.5\ \text{nm}$) is approximately 2000 times larger than the electrostatic force. Again, the electrostatic force is in fact negligible.

However, this simple analysis neglects two key elements of real systems: particle polarizability and surface roughness.

In regard to polarizability, a charged dielectric particle creates an image charge in the conducting surface. The electric field from the image charge then polarizes the particle, which in turn induces further charge on the grounded conducting surface, creating a feedback loop that continues *ad infinitum* [17]. The polarization enhances the attractive electrostatic force. Matsuyama and Yamamoto calculated the electrostatic force for a dielectric particle interacting with a smooth conducting surface for various values of the relative permittivity of the particle, ϵ [18]. They found that charge polarization increased the electrostatic force by an order of magnitude when $\epsilon = 20$, and by two orders of magnitude when $\epsilon = 100$. Thus, particle polarization can be a significant factor in the electrostatic force of a charged particle adhering to a conducting surface.

*daniel.lacks@case.edu

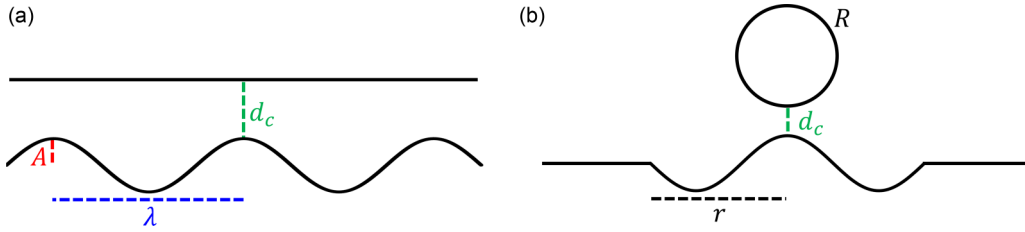


FIG. 1. Schematic of the two systems considered in this study: (a) a flat dielectric slab interacting with a rough conducting and grounded surface and (b) a dielectric sphere interacting with a rough conducting and grounded surface. For presentation purposes we depict the system in 2D, but the simulations were carried out in 3D.

Additionally, all surfaces have some degree of roughness. Many studies have examined the effect of surface roughness on vdW forces in particle adhesion, finding that surface roughness can greatly diminish vdW forces [19–26]. In fact, increasing roughness has been used to intentionally minimize vdW adhesion [16,25,27–29]. The role of surface roughness on electrostatic forces has been studied in the context of electroadhesion [30–34], where potentials are applied to the conducting surface creating an attractive electrostatic force, but we are not aware of studies examining the role of surface roughness in particle adhesion to grounded conducting surfaces.

Surface roughness changes the distances between atoms on the particle and atoms on the surface. If we consider particles sitting on top of asperities, surface roughness acts to make these distances larger. Since vdW forces decay much more rapidly than electrostatic forces with increasing distance, surface roughness can be expected to diminish the vdW forces more than the electrostatic forces. We demonstrate using theoretical analysis that this effect can be significant, and can alter the relative importance of their contributions.

II. METHODOLOGY

We analyze the electrostatic adhesion force in two systems: (A) A flat dielectric slab interacting with a rough conducting and grounded surface. The dielectric slab has permittivity ϵ and uniform surface charge density σ on the bottom surface of the slab. (B) A dielectric sphere interacting with a rough conducting and grounded surface. The sphere has radius, R , permittivity, ϵ , and uniform surface charge density, σ , on the entire surface of the sphere. The particles and surfaces are rigid and do not deform as they interact. We depict these two systems in Fig. 1.

The rough conducting surface is modeled as a sinusoidal landscape,

$$z(x, y) = A \left[\frac{1}{2} \cos(2\pi x/\lambda) + \frac{1}{2} \cos(2\pi y/\lambda) \right], \quad (3)$$

where z is the height of the surface as a function of the coordinates x and y , and A and λ are the amplitude and wavelength of the function describing the surface roughness. For the slab system, the slab is oriented parallel to the rough surface, and separated from the surface by the contact distance, d_c . For the particle system, the particle is situated directly above a peak of the surface, separated by d_c (we consider only this one particle position in order to make the exploration of parameter space feasible). In both cases, we use $d_c = 0.5$ nm. The choice of d_c may significantly affect the vdW force, but it will have

negligible effect on the electrostatic force. The scaling of these forces with d_c is seen most clearly in Eqs. (1) and (2) for a particle contacting a flat surface. For a particle contacting a rough surface the choice of d_c is less significant since the distance between the particle and surface is influenced by the size of the roughness features, rather than d_c alone.

A. Electrostatics force

The electrostatic adhesion force is obtained by first solving Poisson’s equation for the electrostatic potential, using a finite element method with a variable size mesh. We then calculate the adhesion force by integrating the Maxwell stress tensor over either the bottom surface of the flat dielectric slab, or the entire surface of the particle. Due to the symmetry in both systems, the average electric field on the dielectric surface in the x and y directions is 0. Thus, the adhesion force, which is in the z direction, is given by

$$F_E = \iint_S n_z \epsilon_0 \left[E_z^2 - \frac{1}{2} (E_x^2 + E_y^2 + E_z^2) \right] dS, \quad (4)$$

where n_z is the z component of the unit normal vector to the dielectric surface and E_x , E_y , and E_z are the x , y , and z components of the electric field, respectively. Note that while the surface integrals of E_x and E_y are 0, the surface integrals of E_x^2 and E_y^2 are nonzero.

The slab system is constrained using a rectangular calculation cell with side lengths of λ such that the flat surface and rough surface extend to the edges of the cell. The rough surface is the bottom of the cell and has the boundary condition $\phi = 0$, where ϕ is the potential. The sides of the calculation cell have periodic boundary conditions and the top of the slab has the boundary condition $\nabla\phi = 0$. The thickness of the slab is increased until the electrostatic force is converged (i.e., the force is independent of slab thickness).

The particle system is constrained within a cylindrical calculation cell large enough such that the cell boundaries, which have the condition $\nabla\phi = 0$, have negligible impact on the calculation results. Here again the rough surface is the bottom of the cell and has the boundary condition $\phi = 0$. These calculations pose a computational difficulty: as R increases, the particle interacts with a larger area of the rough surface which becomes increasingly computationally intensive to simulate. To expand the regime of R we can feasibly model, we minimize the simulated rough surface area needed for accurate results by modifying the surface as follows. Directly below the particle, we model a circular area with radius r of the rough conducting surface according to Eq. (3). Outside of

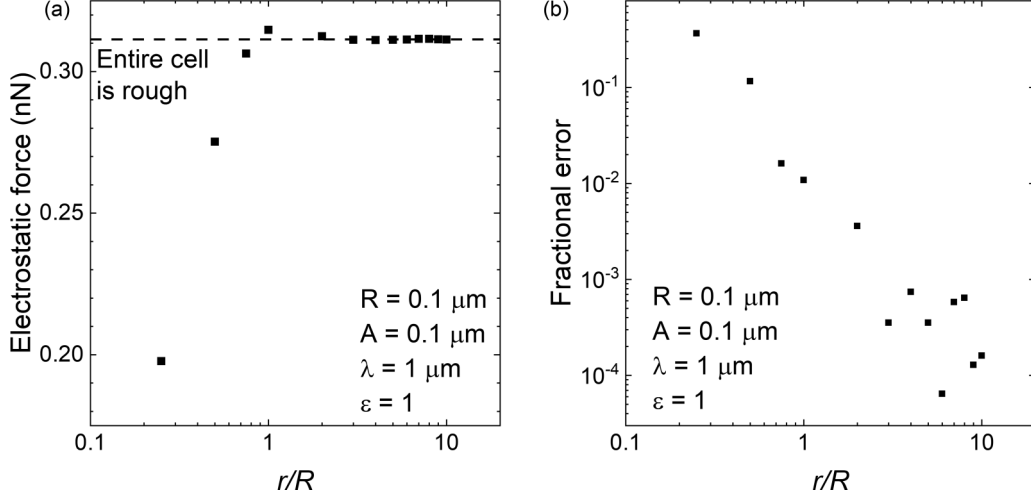


FIG. 2. (a) The electrostatic force and (b) the fractional error as a function of r/R for a particle with $R = 0.1 \mu\text{m}$ and $\varepsilon = 1$ adhering to a rough surface with $A = 0.1 \mu\text{m}$, and $\lambda = 1 \mu\text{m}$. The fractional error is that between the force calculated using the approximation shown in Fig. 1(b), where the radius of the rough surface region is r , and the force calculated when the entire surface in the cell is simulated as a rough surface.

this circular area, we model the surface as a conducting flat surface located at $z = 0$, such that the flat surface is at the average height of the rough surface. This flat surface extends to the boundary of the calculation cell and requires a far less dense mesh to simulate accurately, thereby minimizing computational intensity. This geometry is depicted in Fig. 1(b). We increase the radius r of the inner rough surface described by Eq. (3) until the electrostatic force between the conducting surface and the particle converges (i.e., the force is independent of the area of the inner rough surface). This method works because far from the particle, the size of the roughness features is small relative to the interaction distance, so that this region can be approximated by a flat surface. As shown in Fig. 2 the electrostatic force converges rapidly with increasing r indicating that our approximation has negligible impact on the results.

In both the slab and particle systems, the residual space in the calculation cell is vacuum with permittivity ε_0 . The COMSOL Multiphysics® package is used to carry out the calculations [35]. Our calculation methodology was validated by comparison with known results for the cases of smooth conducting surfaces.

B. van der Waals force

For the slab system, the van der Waals force is calculated using the surface element integration (SEI) method. This method yields the exact solution for the vdW force between a flat surface, and any arbitrarily shaped surface [36]. This

method integrates the vdW interaction between the parallel component of differential surface element dS and the flat surface, which has an analytic solution, over the rough surface. The vdW force F_V calculated from the SEI method is given by

$$F_V = \iint_S \mathbf{n} \cdot \mathbf{k} \frac{F_V^S}{a} dS, \quad (5)$$

where, \mathbf{n} is the outward unit normal vector from the rough surface element dS , \mathbf{k} is the unit vector in the z direction, perpendicular to the flat surface, and $\frac{F_V^S}{a}(h)$ is the vdW force per unit area between two parallel flat surfaces separated by distance h , and is given by, $\frac{F_V^S}{a}(h) = H/6\pi h^3$. Physically, $\mathbf{n} \cdot \mathbf{k} dS$ is the component of rough surface element dS that is parallel to the flat surface. The function for h is the distance between dS on the rough surface and the flat surface and is given as

$$h = d_c - A \left[\frac{1}{2} \cos(2\pi x/\lambda) + \frac{1}{2} \cos(2\pi y/\lambda) \right] + A. \quad (6)$$

Thus, the average vdW force per unit area, a , simplifies to

$$\frac{F_V}{a} = \frac{1}{\lambda^2} \int_{-\frac{\lambda}{2}}^{\frac{\lambda}{2}} \int_{-\frac{\lambda}{2}}^{\frac{\lambda}{2}} \frac{H}{6\pi h^3} dx dy, \quad (7)$$

where h is given by Eq. (6).

For the particle system, we use our previously developed analytic approximation for the vdW force between a particle and a rough surface in the DMT regime of adhesion [24]:

$$F_V = \frac{HR}{6d_c^2} \left(\frac{1}{1 + R/R_a} + \frac{16\pi d_c^2 (R + R_a + d_c)^2}{\lambda^2 (1 + R/R_a)(\lambda^2 + 8d_c(R + R_a + d_c))} \right). \quad (8)$$

Here, R_a is the radius of curvature of asperities and for a sinusoidal surface is given as $R_a = \lambda^2/2\pi^2 A$. This model was derived using the same system geometry used

herein, namely, a spherical particle positioned directly above a peak of a sinusoidal rough surface. Thus, the vdW forces calculated using this model are well suited to

compare to the electrostatic forces we calculate with the above methodology.

III. RESULTS

In the following sections we first characterize the effect of surface roughness on electrostatic adhesion through the ratio F_E/F_E^S , where F_E is the electrostatic force due to a rough conducting surface, and F_E^S is the force due to a smooth conducting surface. Physically, F_E/F_E^S represents the attenuation (if <1) or enhancement (if >1) of the electrostatic adhesion force due to surface roughness. The term F_E/F_E^S does not depend on the charge on the dielectric surface. Then, to determine the effect of roughness on the dominant contribution to adhesion, we calculate the ratio of electrostatic-to-vdW adhesion forces to rough surfaces, F_E/F_V . The term F_E/F_V scales with the ratio σ^2/H in all systems considered in this paper. Here, for concreteness we explicitly consider $\sigma^2/H = 10^9 \text{ C}^2 \text{ m}^{-4} \text{ J}^{-1}$, which corresponds to the physically relevant values $H \sim 10^{-19} \text{ J}$ and $\sigma \sim 10^{-5} \text{ C m}^{-2}$. We emphasize that smaller or larger values of σ^2/H will simply scale F_E/F_V down or up, respectively.

A. Interaction of two surfaces

1. Electrostatic force

We consider the interaction of a charged dielectric surface with a grounded conducting surface, in the limit that both surfaces are infinite in extent. The charged surface will induce an image charge of opposite polarity in the grounded conducting surface such that the electric field within the conductor remains zero. The charged surface electrostatically attracts to this image charge in the conductor.

For flat surfaces, the solution is simple. The resulting image charge is flat and uniform, and the interaction is equivalent to that of two flat surfaces with charges that are equal in magnitude and opposite in polarity. In this case of two flat surfaces, the electrostatic force, F_E^S , per unit area, a , has the simple analytic solution $F_E^S/a = \sigma^2/2\epsilon_0$, which is independent of the separation distance. This solution is also independent of any polarization in the dielectric material (i.e., $\epsilon > 1$). When the conducting surface is flat, polarization in the dielectric surface leads to uniform layers of charge of opposite polarity—since the force due to each of the poles has no distance dependence, the forces from the two poles of the dipole cancel, and thus polarization has no effect on the electrostatic force (when the conducting surface is flat).

We now consider the effects of roughness on electrostatic adhesion. As with the case of flat surfaces, an image charge is induced in the grounded conducting surface. However, roughness causes this induced charge to be nonuniform, such that the charge accumulates in peaks of the surface.

For $\epsilon = 1$, the accumulation of charge in peaks of the conducting surface has no effect on the electrostatic adhesion force. This is because the *total* charge induced in the conducting surface is the same for the rough and flat cases. Since the electrostatic force due to a charged infinite surface does not depend on distance, the distribution of charge on the rough conducting surface does not affect the total force and the electrostatic force is the same for the rough and flat cases.

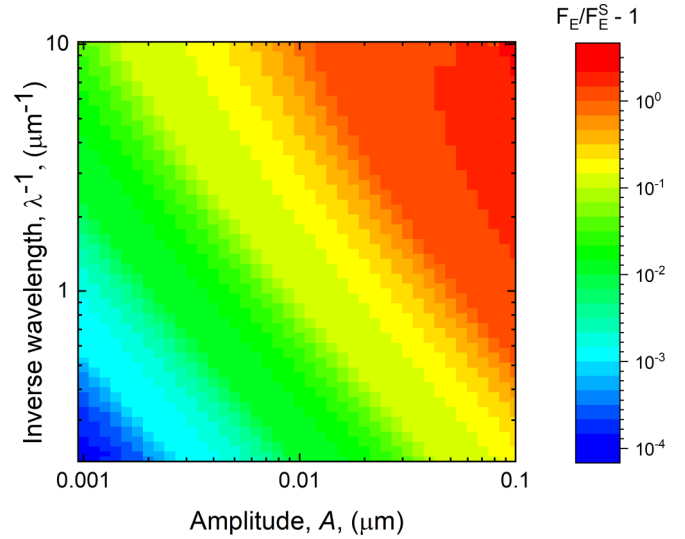


FIG. 3. The enhancement of the electrostatic adhesion force, represented by $F_E/F_E^S - 1$, due to roughness on the conducting surface as a function of roughness amplitude, A , and wavelength, λ . Results are for a dielectric flat slab with $\epsilon = 20$; the dielectric slab has a surface charge, but the ratio F_E/F_E^S is independent of the value of the surface charge.

For $\epsilon > 1$, the situation is not so simple. The accumulation of charge in peaks of the rough conducting surface causes the dielectric surface to polarize more intensely above peaks and less intensely above valleys of the rough surface. In contrast to the case of flat surfaces, the nonuniformity of polarization in the dielectric surface prevents the two poles from canceling each other. Polarization induces further charging of the grounded conducting surface, which further polarizes the dielectric surface, creating a feedback loop that continues *ad infinitum* [17]. Thus, surface roughness enhances the electrostatic adhesion force between the surfaces. This effect is similar to that observed in experimental studies where nonuniform charge distributions on dielectric particles caused enhanced electrostatic adhesion to conducting surfaces [16,37,38].

Figure 3 shows results for the enhancement of the electrostatic adhesion force due to roughness of the conducting surface. We show results for the term $F_E/F_E^S - 1$ for a flat dielectric surface with $\epsilon = 20$ interacting with a grounded conducting surface with sinusoidal roughness characterized by Eq. (3). Physically, positive values of $F_E/F_E^S - 1$ represent the degree of enhancement in electrostatic adhesion due to roughness. As shown in Fig. 3, in the limit of large λ and small A , $F_E/F_E^S - 1$ approaches 0 since the surface becomes flat in these limits. The enhancement of the electrostatic adhesion force is intensified as A increases or λ decreases.

2. Comparison of vdW and electrostatic forces

In Fig. 4 we examine the effect of roughness on the ratio of electrostatic-to-vdW forces, F_E/F_V , for a charged flat dielectric slab with $\epsilon = 20$, and a physically relevant value of σ^2/H . When the conducting surface is flat, the vdW force is seven orders of magnitude greater than the electrostatic force. As shown above, surface roughness enhances the electrostatic

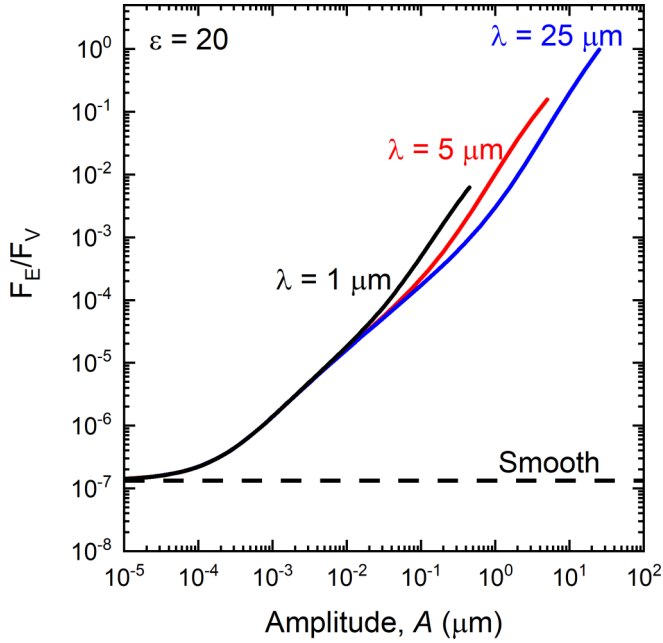


FIG. 4. The ratio of electrostatic to van der Waals forces, F_E/F_V , for a charged flat dielectric surface with $\epsilon = 20$ and $\sigma^2/H = 10^9 \text{ C}^2 \text{ m}^{-4} \text{ J}^{-1}$ in contact with a sinusoidal conducting surface as a function of roughness amplitude, A , for three wavelengths of roughness: $\lambda = 1 \mu\text{m}$ (black), $\lambda = 5 \mu\text{m}$ (red), $\lambda = 25 \mu\text{m}$ (blue), and for a smooth conducting surface (black-dashed).

force on the polarizable slab. However, surface roughness strongly diminishes the vdW force by increasing the interaction distance between the slab and regions of the rough surface. In fact, while the enhancement of the electrostatic force is increased with increasing A and decreasing λ , the vdW force is strongly diminished with increasing A and decreasing λ . For surface roughness features of $\sim 10 \mu\text{m}$, the electrostatic force becomes comparable to the vdW force.

B. Interaction of a particle and a surface

1. Electrostatic force

We address the interaction of a uniformly charged dielectric particle with an infinite grounded conducting surface.

First we consider a nonpolarizable particle ($\epsilon = 1$), and the results are shown in Fig. 5. Unlike the case of two infinite surfaces, the electrostatic force here depends on interaction distance; these results are obtained for $d_c = 0.5 \text{ nm}$. The value of F_E/F_E^S is seen to depend only on the two ratios R/λ and A/λ , rather than on R , A and λ separately.

The ratio R/λ is related to the region of the surface that the particle interacts most strongly with. In the limit $R/\lambda \rightarrow 0$, the surface “appears” flat to the particle, and thus $F_E/F_E^S \rightarrow 1$ in this limit. As R/λ increases from 0, the surface curves away from the particle, thereby causing F_E/F_E^S to decrease. The degree of diminishment depends on the aspect ratio of the asperities, A/λ ; for larger A/λ , the asperity curves away from the particle more quickly causing the electrostatic force to diminish more significantly. As R/λ increases above ~ 1 , increasing particle size brings the particle closer to other asperities, thereby causing F_E/F_E^S to increase with increasing

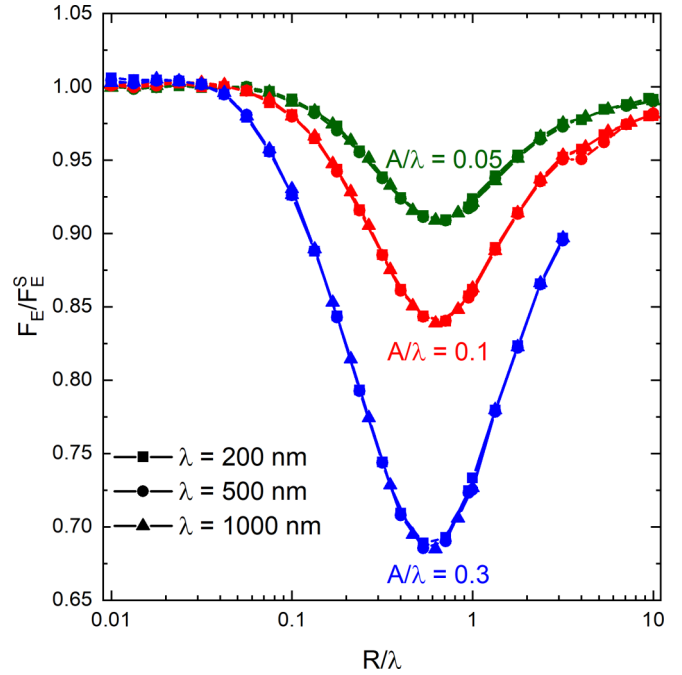


FIG. 5. The effect of roughness on the electrostatic adhesion force, represented by F_E/F_E^S , on an insulating sphere with $\epsilon = 1$ as a function of R/λ for rough surfaces with $A/\lambda = 0.05$ (green), 0.1 (red), and 0.3 (blue). Three different wavelengths of roughness are calculated for each A/λ , $\lambda = 200 \text{ nm}$ (squares), 500 nm (circles), and 1000 nm (triangles). Due to computational limitations, we could not carry out calculations for indefinitely large particle sizes.

R/λ . Due to computational limitations, we could not carry out calculations for indefinitely large particle sizes; however, when R/λ becomes very large, the bottom half of the particle approaches a flat surface and roughness will have no effect on the electrostatic force, as discussed in the previous section.

Now we consider the case of a polarizable particle ($\epsilon > 1$), and results are shown in Fig. 6 for a particle with $\epsilon = 20$. In contrast to the case with $\epsilon = 1$, for $\epsilon > 1$ the value of F_E/F_E^S depends on R , A , and λ separately, rather than just the ratios R/λ and A/λ . Again, due to computational limitations, we could not carry out calculations for indefinitely large particle sizes.

Again, in the limit $R/\lambda \rightarrow 0$, the surface “appears” flat to the particle, and thus $F_E/F_E^S \rightarrow 1$. At finite R/λ , surface roughness has two competing effects. First, as seen in the slab system, charge accumulation in the asperities acts to enhance the electrostatic force for $\epsilon > 1$. Second, as seen in the particle system with $\epsilon = 1$, surface roughness increases the separation distance from the particle to regions of the surface, which diminishes the electrostatic force. The first effect dominates for smaller R/λ and the second effect dominates for larger R/λ . Furthermore, both effects increase in magnitude with larger A and smaller λ .

The general behavior for polarizable particles is that surface roughness causes electrostatic adhesion to be enhanced at small R/λ , diminished at intermediate R/λ , and independent of surface roughness at large R/λ . As seen in Fig. 7, increased permittivity acts to shift the transitions between these regimes to larger R/λ . For particles with high permittivity (e.g.,

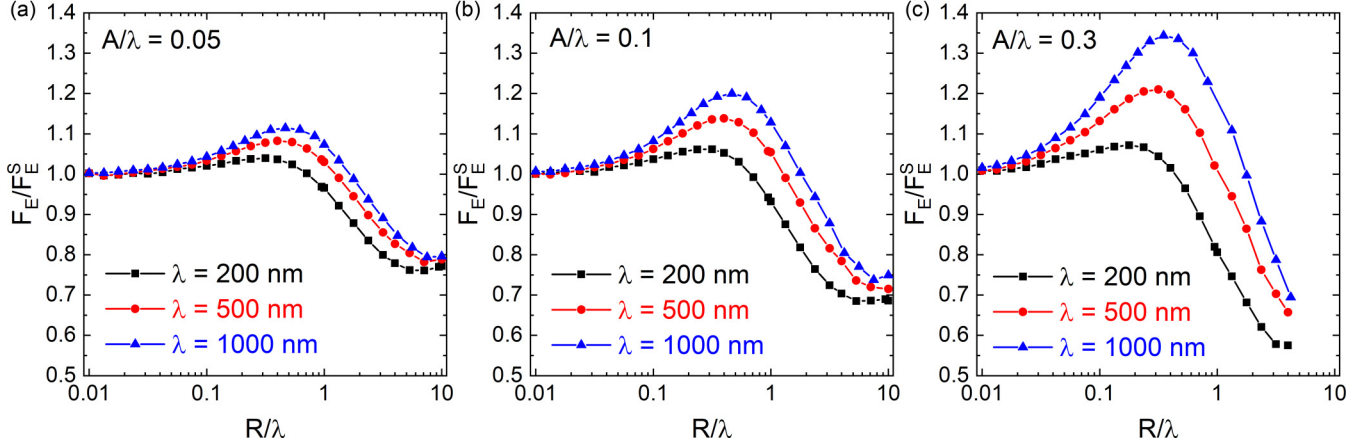


FIG. 6. The effect of surface roughness on the electrostatic adhesion force, represented by F_E/F_E^S , on a dielectric sphere with $\varepsilon = 20$ as a function of R/λ for rough surfaces with (a) $A/\lambda = 0.05$, (b) $A/\lambda = 0.1$, and (c) $A/\lambda = 0.3$. Three different wavelengths of substrate roughness are calculated for each A/λ , $\lambda = 200$ nm (black squares), 500 nm (red circles), and 1000 nm (blue triangles). Due to computational limitations, we could not carry out calculations for indefinitely large particle sizes.

$\varepsilon = 20$), the transition to the large R/λ regime gets shifted to values of R/λ that are beyond the computational limitations of our methodology.

2. Comparison of vdW and electrostatic forces

Figure 8 shows the ratio of electrostatic to vdW forces, F_E/F_V , as a function of particle size, with a physically relevant value of σ^2/H . For rough surfaces, we note again that computational limitations preclude rigorous calculation of the electrostatic force for larger particle sizes (which is why the solid lines in Fig. 8 stop). However, we can use an approx-

imation to extend the range of our analysis. Since surface roughness changes electrostatic forces by only around a factor of two while changing vdW forces by orders of magnitude, we can use the approximation $F_E \approx F_E^S$ when comparing the two forces. The dotted lines in Fig. 8 depict results using this approximation. From a comparison in the regime where we have rigorous calculations, we see that the approximation is indeed accurate for our purpose.

In general, electrostatic forces are completely negligible for very small particles—e.g., the electrostatic force is only $\sim 10^{-5}$ that of the vdW forces for particles sized ~ 10 nm. However, the significance of the electrostatic force increases with particle size, in a way that depends on particle polarizability and surface roughness.

First, we consider the behavior for smooth surfaces. For a nonpolarizable particle, the electrostatic force only becomes comparable to the vdW force as the particle size increases to around a millimeter. Polarizability increases the electrostatic contribution, and for $\varepsilon = 20$ the electrostatic force becomes comparable to the vdW force as the particle size increases to around $100 \mu\text{m}$.

Surface roughness has a dramatic effect on the relative contributions of the two forces. We examine here physically reasonable rough surfaces, with roughness amplitudes and wavelengths in the hundreds of nm. For a nonpolarizable particle, physically reasonable surface roughness can cause the electrostatic force to become comparable to the vdW force at $R \sim 10\text{--}20 \mu\text{m}$. For a polarizable particle with $\varepsilon = 20$, the electrostatic force becomes comparable to the vdW force at $R \sim 3\text{--}7 \mu\text{m}$.

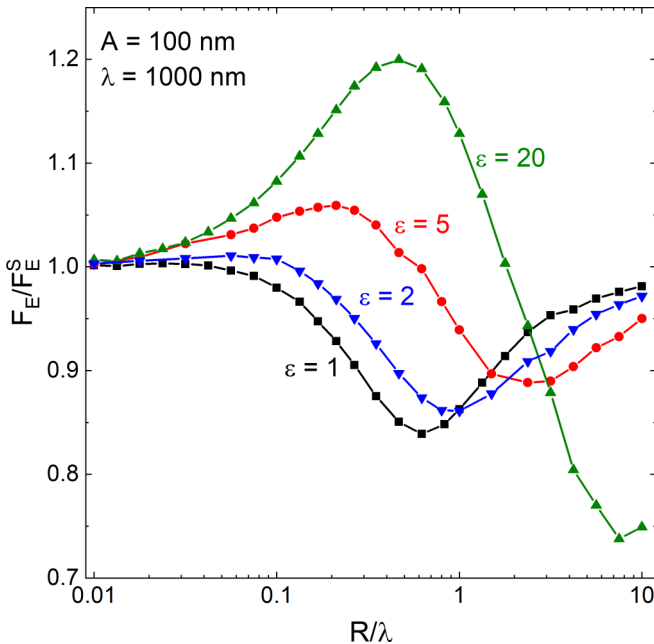


FIG. 7. The effect of surface roughness on the electrostatic adhesion force, represented by F_E/F_V^S , on spheres with $\varepsilon = 1$ (black), 2 (blue), 5 (red), and 20 (green) as a function of R/λ for a rough surface with $A = 100$ nm and $\lambda = 1000$ nm.

IV. DISCUSSION

In systems of small particles, often called dusts, the particle mass is so small that the forces of gravity can be easily overcome by other forces— aerodynamic forces can loft the particles, and adhesive forces can cause the particles to adhere to surfaces. These effects become significant for particles

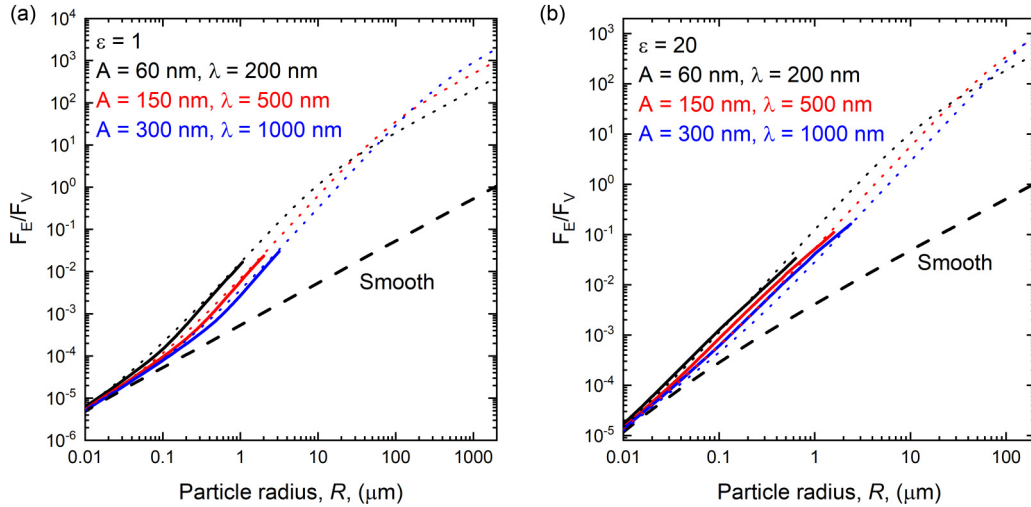


FIG. 8. The ratio of electrostatic to van der Waals adhesion force, F_E/F_V , for a dielectric particle with (a) $\epsilon = 1$ and (b) $\epsilon = 20$. The results are obtained with $\sigma^2/H = 10^9 \text{ C}^2 \text{ m}^{-4} \text{ J}^{-1}$. Three rough substrates were considered: $A = 60 \text{ nm}$ and $\lambda = 200 \text{ nm}$ (black); $A = 150 \text{ nm}$ and $\lambda = 500 \text{ nm}$ (red); and $A = 300 \text{ nm}$ and $\lambda = 1000 \text{ nm}$ (blue). The electrostatic forces were calculated using the numerical methodology (solid lines) and analytic approximations (dotted lines). The analytic approximations of F_E/F_V were calculated by the ratio of (a) Eqs. (2) and (8), and (b) the empirical fit from Matsuyama and Yamamoto [18] for the electrostatic force between a polarizable sphere and a flat surface and Eq. (8). The rough substrate F_E/F_V is compared with that of a smooth substrate represented by the black-dashed line.

smaller than $\sim 100 \mu\text{m}$, and become very important for particles smaller than $\sim 10 \mu\text{m}$.

It is commonly assumed that the adhesive forces which cause these small particles to stick to surfaces are dominated by the vdW force. As shown above, this is clearly the case for smooth surfaces, where the vdW forces are ~ 100 times larger than electrostatic forces. In this case, electrostatic forces can be neglected when considering particle adhesion.

However, our results show that for rough surfaces, electrostatic forces can be significant and therefore must not be neglected. The reason for this is that the electrostatic and vdW forces scale differently with distance r —electrostatic forces scale as $1/r^2$, while vdW forces scale as $1/r^7$. Surface roughness effectively increases the interaction distances between the particle and surface, and thus the vdW force diminishes much more strongly due to roughness than the electrostatic force. This difference in scaling has been exploited to enhance the contribution of electrostatic forces in toner particles by intentionally increasing the roughness of the dielectric particles [28,29,38,39]. Our results indicate that a similar effect occurs due to roughness of the conducting surface.

The well-defined system of a uniformly charged, nondeformable (DMT limit) spherical particle adhering directly above a peak of a sinusoidal surface enables us to clearly discern the effect of roughness and particle polarization on the adhesive forces. While real systems have irregular particle and surface morphology [40–42], material deformation [20,43], and nonuniform charge distribution [42,43], we nonetheless expect our qualitative conclusions to apply to real systems. Most importantly, we show that surface roughness can cause F_E/F_V to vary by several orders of magnitude. In comparison, the difference in the adhesion force between highly deformable (Johnson, Kendall, Roberts limit) and rigid (DMT limit) particles is typically less than $\sim 30\%$ [20,44,45]. Similarly, the adhesion forces predicted by models assuming highly simplified systems [26,46] typically differ by less than

$\sim 50\%$ from experimental adhesion forces wherein the surfaces are random with several length scales of roughness [21,26,47–50].

We considered a particle positioned directly above a peak of the rough surface in order to reduce the parameter space to examine; here we address the effects of particle position. For $R > \lambda$, the position of the particle on the surface is not important since the particle will always contact the peaks of the surface, and the present results are generally applicable. In contrast, for $R < \lambda$, the position of the particle is important. In our sinusoidal model, the vdW force decreases with increasing surface roughness when the particle sits above a peak, but the vdW force increases with increasing surface roughness when the particle sits in a valley (because more of the surface becomes closer to the particle). Therefore, surface roughness would not increase the relative contribution of electrostatic interactions in the case that $R < \lambda$ and the particle is situated in a valley.

Furthermore, our conclusions regarding the relative importance of electrostatic forces depend strongly on the surface charge density σ . We note that the charge density on surfaces has been reported with values of $\sim 10^{-6}$ [51,52], $\sim 10^{-5}$ [53,54], $\sim 10^{-4}$ [7,55–57], and $\sim 10^{-3} \text{ C m}^{-2}$ [58]. As discussed earlier, F_E/F_V for a given system can be well approximated using analytic expressions by estimating that $F_E \approx F_E^S$. Thus, for a nonpolarizable particle F_E/F_V can be approximated from the ratio between Eqs. (2) and (8). For a polarizable particle, the empirical fit from Matsuyama and Yamamoto [18] for the electrostatic force between a polarizable sphere and a flat surface can be used in place of Eq. (2) above.

V. CONCLUSION

In summary, here we characterize the effect of polarization and surface roughness on electrostatic adhesion to a conducting surface. We find that unlike van der Waals forces,

which decay by orders of magnitude due to surface roughness, electrostatic forces are only slightly diminished and in some cases are enhanced by roughness. As a result, surface roughness and polarization increase the contribution of electrostatic forces to adhesion by several orders of magnitude and greatly reduce the particle size where electrostatic forces are comparable to van der Waals forces.

ACKNOWLEDGMENTS

This project was supported from the Institut de Radioprotection et de Sûreté Nucleaire and from the U.S. National Science Foundation (NSF) under Grants No. 1559508 and No. 1604909.

- [1] S. I. Krasheninnikov, A. Y. Pigarov, R. D. Smirnov, M. Rosenberg, Y. Tanaka, D. J. Benson, T. K. Soboleva, T. D. Rognlien, D. A. Mendis, B. D. Bray, D. L. Rudakov, J. H. Yu, W. P. West, A. L. Roquemore, C. H. Skinner, J. L. Terry, B. Lipschultz, A. Bader, R. S. Granetz, C. S. Pitcher, N. Ohno, S. Takamura, S. Masuzaki, N. Ashikawa, M. Shiratani, M. Tokitani, R. Kumazawa, N. Asakura, T. Nakano, A. M. Litnovsky, and R. Maqueda, *Plasma Phys. Control. Fusion* **50**, 124054 (2008).
- [2] G. Hendrickson, *Chem. Eng. Sci.* **61**, 1041 (2006).
- [3] A. Sowinski, A. Mayne, and P. Mehrani, *Chem. Eng. Sci.* **71**, 552 (2012).
- [4] J. Yao, Y. Zhang, C. H. Wang, S. Matsusaka, and H. Masuda, *Ind. Eng. Chem. Res.* **43**, 7181 (2004).
- [5] N. Susanti and H. Grosshans, *Adv. Powder Technol.* **31**, 3597 (2020).
- [6] D. A. Hays, *J. Adhes.* **51**, 41 (1995).
- [7] E. Chung, S. Yiaccoumi, I. Lee, and C. Tsouris, *Environ. Sci. Technol.* **44**, 6209 (2010).
- [8] K. A. McCarthy, D. A. Petti, W. J. Carmack, and G. R. Smolik, *Fusion Eng. Des.* **42**, 45 (1998).
- [9] C. Grisolia, E. Hodille, J. Chene, S. Garcia-Argote, G. Pieters, A. El-Kharbachi, L. Marchetti, F. Martin, F. Miserque, D. Vrel, M. Redolfi, V. Malard, G. Dinescu, T. Acsente, F. Gensdarmes, S. Peillon, B. Pegourié, and B. Rousseau, *J. Nucl. Mater.* **463**, 885 (2015).
- [10] A. El-Kharbachi, J. Chêne, S. Garcia-Argote, L. Marchetti, F. Martin, F. Miserque, D. Vrel, M. Redolfi, V. Malard, C. Grisolia, and B. Rousseau, *Int. J. Hydrogen Energy* **39**, 10525 (2014).
- [11] R. A. Bowling, in *Particles on Surfaces I: Detection, Adhesion, and Removal*, edited by K. L. Mittal (Springer, Boston, MA, 1988), pp. 129–42.
- [12] K. L. Mittal and R. Jaiswal, *Particle Adhesion and Removal* (Wiley, Hoboken, NJ, 2015).
- [13] R. A. Bowling, *J. Electrochem. Soc.* **132**, 2208 (1985).
- [14] M. Soltani and G. Ahmadi, *J. Adhes. Sci. Technol.* **8**, 763 (1994).
- [15] J. Israelachvili, *Intermolecular and Surface Forces*, 3rd ed. (Academic Press, New York, 2011).
- [16] D. A. Hays, *J. Adhes. Sci. Technol.* **9**, 1063 (1995).
- [17] W. Y. Fowlkes and K. S. Robinson, in *Particles on Surfaces I: Detection, Adhesion, and Removal*, edited by K. L. Mittal, (Springer, Boston, MA, 1988), pp. 143–55.
- [18] T. Matsuyama and H. Yamamoto, *KONA Powder Part. J.* **16**, 223 (1998).
- [19] H. Krupp, *Adv. Colloid Interface Sci.* **1**, 111 (1967).
- [20] D. Tabor, *J. Colloid Interface Sci.* **58**, 2 (1977).
- [21] Y. I. Rabinovich, J. J. Adler, A. Ata, R. K. Singh, and B. M. Moudgil, *J. Colloid Interface Sci.* **232**, 17 (2000).
- [22] E. R. Beach, G. W. Tormoen, J. Drelich, and R. Han, *J. Colloid Interface Sci.* **247**, 84 (2002).
- [23] K. Cooper, A. Gupta, and S. Beaudoin, *J. Colloid Interface Sci.* **234**, 284 (2001).
- [24] S. Rajupet, M. Sow, and D. J. Lacks, *Phys. Rev. E* **102**, 012904 (2020).
- [25] S. N. Ramakrishna, L. Y. Clasohm, A. Rao, and N. D. Spencer, *Langmuir* **27**, 9972 (2011).
- [26] J. Katainen, M. Paajanen, E. Ahtola, V. Pore, and J. Lahtinen, *J. Colloid Interface Sci.* **304**, 524 (2006).
- [27] T. Kim, C. Min, M. Jung, J. Lee, C. Park, and S. Kang, *Appl. Surf. Sci.* **389**, 889 (2016).
- [28] H. Iimura, H. Kurosu, and T. Yamaguchi, *NIP Digit. Fabr. Conf.* **1999**, 535 (1999).
- [29] H. Iimura, H. Kurosu, and T. Yamaguchi, *J. Imaging Sci. Technol.* **44**, 457 (2000).
- [30] B. N. J. Persson and J. Guo, *Soft Matter* **15**, 8032 (2019).
- [31] M. Ayyildiz, M. Scaraggi, O. Sirin, C. Basdogan, and B. N. J. Persson, *Proc. Natl. Acad. Sci.* **115**, 12668 (2018).
- [32] B. N. J. Persson, *J. Chem. Phys.* **148**, 144701 (2018).
- [33] B. N. J. Persson, M. Scaraggi, A. I. Volokitin, and M. K. Chaudhury, *EPL (Europhysics Lett.)* **103**, 36003 (2013).
- [34] M. S. Lhernould, A. Delchambre, S. Régnier, and P. Lambert, *Appl. Surf. Sci.* **253**, 6203 (2007).
- [35] COMSOL Multiphysics® v. 5.4. www.comsol.com. COMSOL AB, Stockholm, Sweden.
- [36] S. Bhattacharjee and M. Elimelech, *J. Colloid Interface Sci.* **193**, 273 (1997).
- [37] D. A. Hays, in *Particles on Surfaces I: Detection, Adhesion, and Removal*, edited by K. L. Mittal (Springer, Boston, MA, 1988), pp. 351–60.
- [38] D. A. Hays and J. C. Shefflin, *J. Electrostat.* **63**, 687 (2005).
- [39] H. Zhou, M. Götzinger, and W. Peukert, *Powder Technol.* **135–136**, 82 (2003).
- [40] B. N. J. Persson and M. Scaraggi, *J. Chem. Phys.* **141**, 124701 (2014).
- [41] C. Q. LaMarche, S. Leadley, P. Liu, K. M. Kellogg, and C. M. Hrenya, *Chem. Eng. Sci.* **158**, 140 (2017).
- [42] S. Eichenlaub, A. Gelb, and S. Beaudoin, *J. Colloid Interface Sci.* **280**, 289 (2004).
- [43] K. L. Johnson, K. Kendall, and A. D. Roberts, *Proc. R. Soc. A Math. Phys. Eng. Sci.* **324**, 301 (1971).
- [44] P. Prokopovich and S. Perni, *Colloids Surfaces A Physicochem. Eng. Asp.* **383**, 95 (2011).

- [45] K. L. Johnson and J. A. Greenwood, *J. Colloid Interface Sci.* **192**, 326 (1997).
- [46] Y. I. Rabinovich, J. J. Adler, A. Ata, R. K. Singh, and B. M. Moudgil, *J. Colloid Interface Sci.* **232**, 10 (2000).
- [47] A. Kumar, T. Staedler, and X. Jiang, *J. Colloid Interface Sci.* **409**, 211 (2013).
- [48] O. Laitinen, K. Bauer, J. Niinimäki, and U. A. Peuker, *Powder Technol.* **246**, 545 (2013).
- [49] S. Peillon, A. Autricque, M. Redolfi, C. Stancu, F. Gensdarmes, C. Grisolia, and O. Pluchery, *J. Aerosol Sci.* **137**, 105431 (2019).
- [50] S. Matope, Y. I. Rabinovich, and A. F. Van der Merwe, *Colloids Surfaces A Physicochem. Eng. Asp.* **411**, 87 (2012).
- [51] V. Lee, N. M. James, S. R. Waitukaitis, and H. M. Jaeger, *Phys. Rev. Materials* **2**, 035602 (2018).
- [52] A. E. Wang, I. Greber, and J. C. Angus, *J. Electrostat.* **101**, 103359 (2019).
- [53] X. Shen, A. E. Wang, R. M. Sankaran, and D. J. Lacks, *J. Electrostat.* **82**, 11 (2016).
- [54] T. Matsuyama, M. Ogu, H. Yamamoto, J. C. M. Marijnissen, and B. Scarlett, *Powder Technol.* **135–136**, 14 (2003).
- [55] T. Miura and I. Arakawa, *IEEE Trans. Dielectr. Electr. Insul.* **14**, 560 (2007).
- [56] T. Matsuyama and H. Yamamoto, *J. Phys. D. Appl. Phys.* **30**, 2170 (1997).
- [57] G. A. Cottrell, *J. Phys. D. Appl. Phys.* **11**, 681 (1978).
- [58] R. G. Horn and D. T. Smith, *Science* **256**, 362 (1992).